



STUDY OF ASPHALTENE PRECIPITATION-DEPOSITION DUE TO PRESSURE DEPLETION

^aPiroozan, Z. ¹; ^bKharrat, R.; ^bEmamzadeh, A.

^aDepartment of Chemical and Petroleum Engineering, Islamic Azad University

^bPetroleum University of Technology, Petroleum Research Center, Tehran, Iran

ABSTRACT

The purpose of this study is to model the effects of asphaltene precipitation and deposition on fluid flow and oil production at reservoir conditions, in order to provide a better understanding of the main parameters that may enhance asphaltene precipitation or deposition. PVT data were matched with the Peng-Robinson equation of state, and a pure solid model was used to represent the asphaltene precipitation. Sensitivity analysis was done to understand the effects of some experimental parameters, such as the surface deposition rate coefficient (α) and the entrainment rate coefficient (β), on asphaltene precipitation and deposition. In addition, the effects of oil production rate on asphaltene precipitation and deposition was investigated. Based on this study, controlling production rate of the wells was found to be an important strategy in delaying the problem of asphaltene precipitation.

KEYWORDS

asphaltene; precipitation; deposition; flocculation; sensitivity analysis

¹ To whom all correspondence should be addressed.

Address: Department of Chemical and Petroleum Engineering, Islamic Azad University-Science & Research Branch, Hesarak, Tehran, Iran
Telephone: +989133409776 | e-mail: z.piroozan@gmail.com

1. INTRODUCTION

Asphaltene precipitation-deposition causes serious problems in the oil industry. Variation of oil composition, reservoir pressure and temperature are reported to be the most important factors that influence asphaltene precipitation from reservoir oil (Garrouch, 2003; Hirschberg et al., 1984; Jamshidnezhad, 2005; Kohse et al., 2004; Nghiem, 2000; Sarma, 2003).

When pressure in the reservoir is reduced the colloidal suspension may become destabilized, resulting in asphaltene and resin molecules precipitating out of the oil phase. They may continue to flow as suspended particles, or they may deposit on to the rock surface causing plugging and wettability alteration. Deposition begins with adsorption of flocculated asphaltene particles on to active sites on the rock surface, particularly on to clayey minerals with high specific area, such as kaolinites. This is followed by hydrodynamic retention or trapping process of particles at the pore throats (Leontaritis, 1994; Moghadasi et al., 2006; Nghiem, 2000). Deposition of solid asphaltenes causes a reduction of the pore space available for fluids (Nghiem, 2000). It is also possible that deposited asphaltene particles may be re-entrained in the flowing oil stream due to mechanical erosion or ablation effects if the interstitial velocity of the fluids becomes high enough (Bruce et al., 2004).

This paper simulates asphaltene precipitation and deposition in an oil reservoir due to primary depletion that was implemented in a compositional reservoir simulator. The goal of this study is to model the effects of asphaltene precipitation and deposition on fluid flow and oil production and also to understand the effect of surface deposition rate coefficient (α), the entrainment rate coefficient (β), the pore throat plugging rate coefficient (γ) and the critical interstitial velocity (v_c) on asphaltene precipitation and deposition with sensitivity analysis from the oil reservoir.

2. EXPERIMENTAL DATA

The experimental PVT data include compositional analysis, constant composition expansion, differential liberation, and separator

Table 1. Reservoir fluids composition (Before lumping).

| Component | Well 1 %mol | Well 2 %mol | Well 3 %mol |
|---------------------------------|-------------|-------------|-------------|
| H ₂ S | 1.93 | 0.02 | 0 |
| CO ₂ | 0.01 | 2.07 | 1.74 |
| N ₂ | 1.83 | 0.13 | 0.39 |
| C ₁ | 10.5 | 17.1 | 20.6 |
| C ₂ | 7.42 | 8.05 | 7.31 |
| C ₃ | 6.18 | 6.88 | 5.34 |
| IC ₄ | 1.43 | 1.33 | 1 |
| NC ₄ | 5.07 | 4.43 | 3.65 |
| IC ₅ | 2.53 | 2.38 | 3.1 |
| NC ₅ | 3.22 | 2.79 | 4.75 |
| C ₆ | 3.91 | 3.35 | 5.48 |
| C ₇₊ /C ₇ | 56 | 3.03 | 3.23 |
| C ₈ | – | 1.6 | 1.32 |
| C ₉ | – | 0.81 | 2.27 |
| C ₁₀ | – | 1.67 | 2.19 |
| C ₁₁ | – | 2.62 | 1.81 |
| C ₁₂₊ | – | 41.8 | 35.9 |

test and saturation pressure data. Asphaltene precipitation data consist of measurements of onset pressures of three wells and also some important parameters that control asphaltene precipitation, flocculation and deposition.

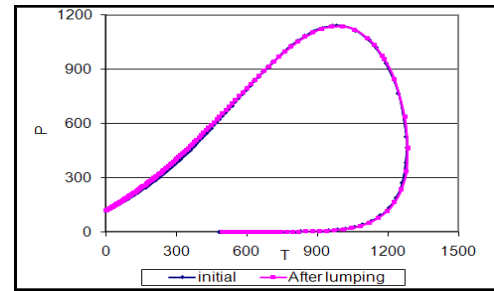
2.1 PVT model construction

The reservoir fluid components are given in Table 1. The oil phase is modeled with the Peng-Robinson equation of state. The initial model of the fluid is generated by splitting and lumping the components (Table 2). Lumped component properties are generated using the Lee-Kesler mixing rules. The adequacy of the lumping scheme is checked by generating phase envelopes for both the initial component and lumped models. As shown in Figure 1, the phase envelopes are nearly identical for the two cases.

After component lumping, a procedure for matching PVT data was done. Figure 2 shows good agreement between experimental and calculated data for oil viscosity, gas viscosity, gas-oil ratio, relative oil volume, gas compressibility factor, gas formation volume factor, gas specific gravity, oil specific gravity, and constant composition expansion.

Table 2. Reservoir fluids composition (After lumping).

| Component | Well 1 %mol | Well 2 %mol | Well 3 %mol |
|------------------------------------|----------------|----------------|----------------|
| H ₂ S | 0.000197 | 0 | 0.0193 |
| CO ₂ | 0.0203 | 0.0174 | 0.0001 |
| N ₂ | 0.00128 | 0.0039 | 0.0183 |
| C ₁ | 0.168 | 0.205 | 0.105 |
| C ₂ | 0.0791 | 0.0731 | 0.0742 |
| C ₃ | 0.0676 | 0.0534 | 0.0618 |
| IC ₄ | 0.0131 | 0.01 | 0.0143 |
| NC ₄ | 0.0435 | 0.0365 | 0.0507 |
| IC ₅ | 0.0234 | 0.031 | 0.0253 |
| NC ₅ | 0.0274 | 0.0475 | 0.0322 |
| FC ₆ | 0.0329 | 0.0548 | 0.0391 |
| C ₇ | 0.0298 | 0.0323 | 0.0388 |
| C ₈ | 0.0157 | 0.0132 | 0.0361 |
| C ₉ | 0.00796 | 0.0227 | 0.0336 |
| C ₁₀ | 0.0164 | 0.0219 | 0.0313 |
| C ₁₁ | 0.0257 | 0.0181 | 0.0291 |
| C ₁₂ to C ₁₅ | 0.0888 | 0.084 | 0.0976 |
| C ₁₆ to C ₂₀ | 0.0845 | 0.0779 | 0.0884 |
| C ₂₁ to C ₂₅ | 0.0623 | 0.0558 | 0.0618 |
| C ₂₆ to C ₃₀ | 0.046 | 0.04 | 0.0431 |
| C _{31A} ⁺ | 0.127 | 0.067 | 0.0731 |
| C _{31B} ⁺ | 0.019 | 0.034 | 0.0268 |


Figure 1. Phase envelope.

maximum amount of precipitation is located on a region around the bubble point pressure. Below the saturation pressure, precipitated solids can re-dissolve in the liquid phase. This phenomenon has been observed in the laboratory for pressure depletion. As a result of gas liberation from the oil phase, the solubility parameter of the liquid phase will be changed, allowing for re-dissolution of the precipitated asphaltene (Nghiem and Dennis, 1996). It is possible that all of the precipitated asphaltene will go back into solution at sufficiently low pressures.

2.3 Dynamic model construction

The reservoir consists of $50 \times 22 \times 5$ grid blocks in the x, y and z directions respectively. Petrophysical properties are given in Table 3. Figure 4 shows a schematic of the model reservoir. Well properties are given in Table 4.

2.2 Asphaltene/wax modeling

The procedure for modeling the precipitation of asphaltene from recombined live oil reservoirs due to pressure depletion was done by selecting the exact onset pressure and a pressure point above saturation pressure, at which a small amount of asphaltene precipitate is determined. The asphaltene precipitation plot was generated as shown in Figure 3. It can be observed that the

Table 3. Petrophysical properties.

| Property | Value |
|---------------------|-------|
| Permeability x (md) | 250 |
| Permeability y (md) | 250 |
| Permeability z (md) | 100 |
| Porosity | 18 % |

Table 4. Well properties.

| | Well 1 | Well 2 | Well 3 |
|---|--------|--------|--------|
| Formation | Sarvak | Sarvak | Sarvak |
| GOR (SCF/STB) | 266.8 | 292.1 | 361.69 |
| Reservoir Pressure (psia) | 4600 | 4600 | 4470 |
| Molecular weight of C+7/C+12 | 285 | 390 | 370 |
| Specific gravity of C+7/C+12 fraction at 15.5 °C | 0.9347 | 0.9634 | 0.9769 |
| Asphaltene content in stock tank oil, wt% | 9.3 | 6.3 | 12.8 |
| Bubble point at 96 °C | 1139 | 1090 | 1432 |
| Reservoir temperature, °C | 96 | 96 | 96 |
| °API | 19.5 | 20.14 | 20.37 |

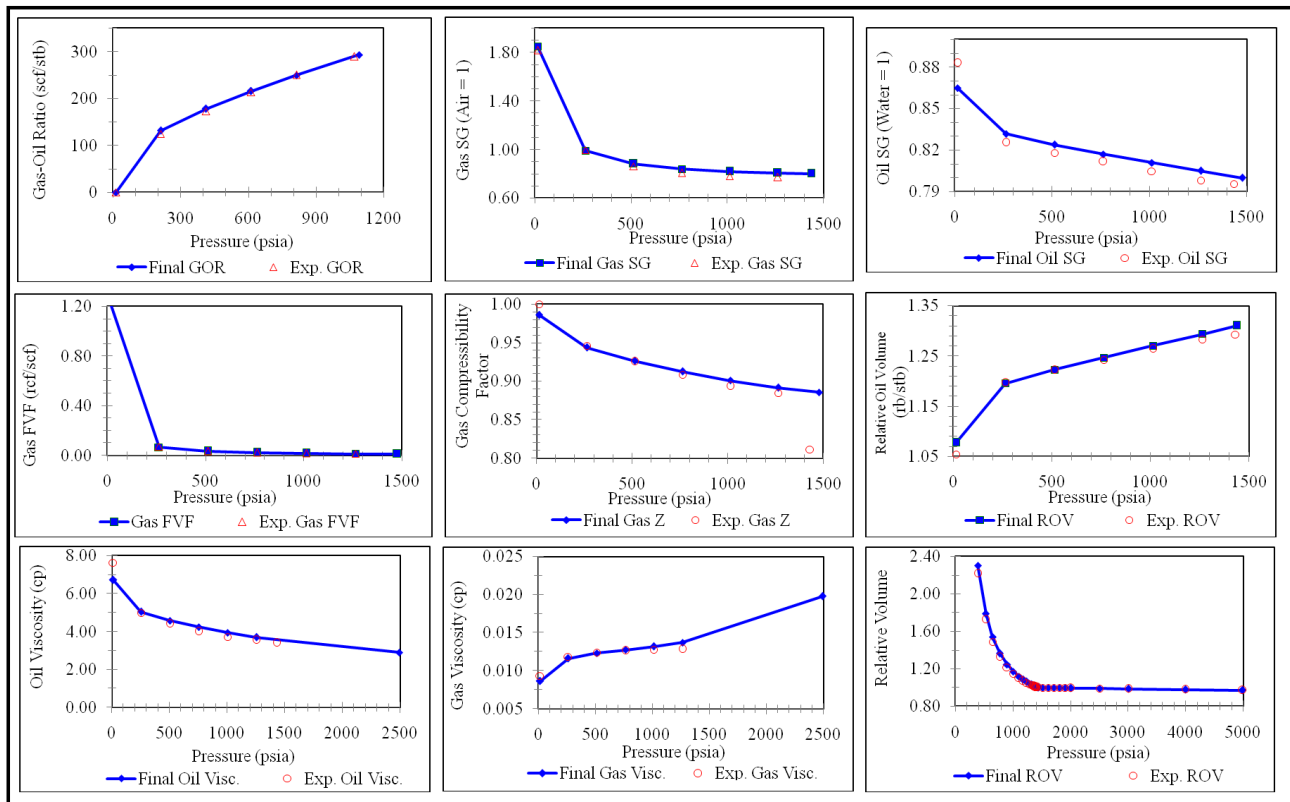


Figure 2. Procedures for matching PVT data.

3. RESULTS AND DISCUSSION

3.1 Asphaltene precipitation versus production

Asphaltene precipitation versus production at different saturation pressures are given in Figures 5 through 7. As can be seen, by decreasing pressure the asphaltene precipitation increases, and maximum amount of precipitation occurs around the bubble point pressure, with the liberation of gas from the oil at the saturation pressure. The

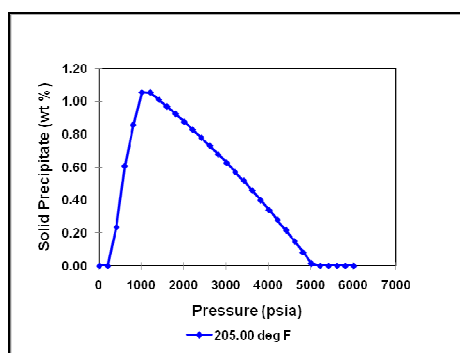


Figure 3. The asphaltene precipitation plot.

results are in agreement with laboratory experiments and field observations.

3.2 Sensitivity analysis

The solid deposition model comprises some parameters that control the deposition of flocculated solid particles. Sensitivity analysis was done to investigate the effect of each parameter on asphaltene precipitation, flocculation and deposition. These parameters are the surface deposition rate coefficient (α), the entrainment rate coefficient (β), the pore throat plugging rate

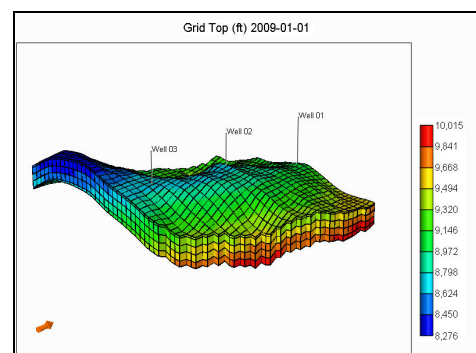
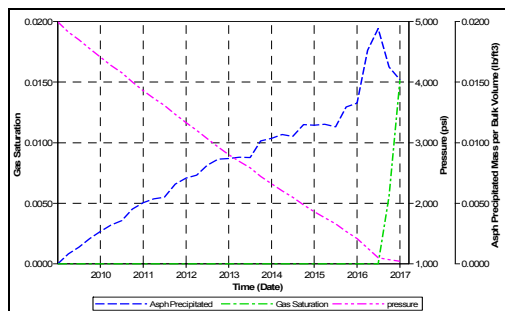


Figure 4. 3-D schematic of the reservoir.

Table 5. Experimental parameters of the asphaltene samples.

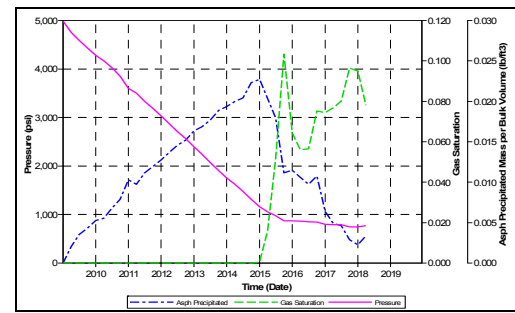
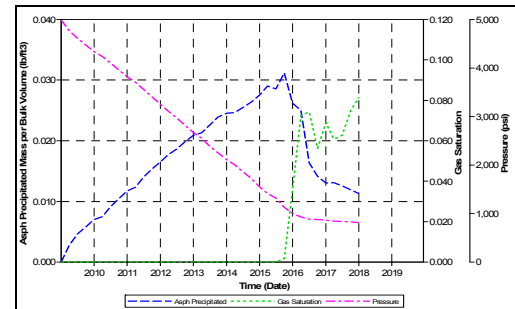
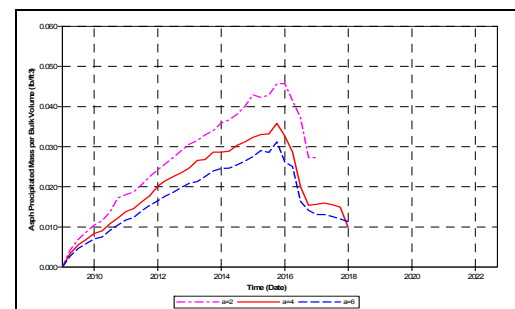
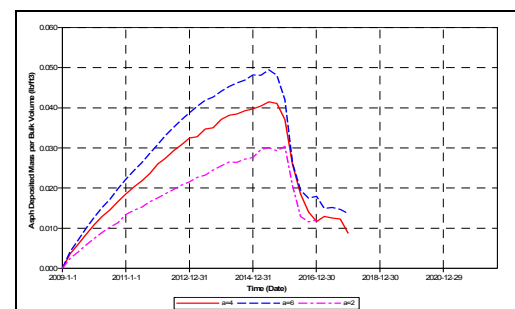
| Parameter | Value |
|--------------------------|-------|
| k_{12} (1/day) | 0.8 |
| k_{21} (1/day) | 0.2 |
| α (1/day) | 4.64 |
| β (1/m) | 0.62 |
| γ (1/m) | 1.21 |
| σ (Dimensionless) | 64.75 |
| v_c (ft/day) | 8.64 |
| R_f Exponent | 3 |

coefficient (γ) and the critical interstitial velocity (v_c). Experimental data were used to validate the deposition model, and were altered in order to investigate the effect of each parameter on asphaltene precipitation, flocculation and deposition. The experimental parameters of the asphaltene samples (Kharrat et al., 2009) are given in Table 5.


Figure 5. Asphaltene precipitation versus production (Saturation pressure = 1090 psia).

3.3 Effect of surface deposition rate coefficient

Figures 8 through 11 illustrate the effect of surface deposition rate coefficient on asphaltene precipitation, deposition, oil resistance factor and permeability reduction. The effect of α on asphaltene precipitation and deposition are shown in Figures 8 and 9, respectively. By increasing α , asphaltene precipitation decreases. On the other hand the asphaltene deposition increases as the value of α increases. Figure 10 shows the effect of α on the oil resistance factor. Once the solid phase has adsorbed on the reservoir rock, partial plugging of the formation is expected, so with increasing α the oil resistance factor increases. Figure 11 shows the effect of α on the permeability reduction. It shows that permeability reduction increases with increasing α .


Figure 6. Asphaltene precipitation versus production (Saturation pressure = 1139 psia).

Figure 7. Asphaltene precipitation versus production (Saturation pressure = 1432 psia).

Figure 8. Effect of α on asphaltene precipitation.

Figure 9. Effect of α on asphaltene deposition.

Based on these results, as the amount of precipitated asphaltene decreases, the amount of deposited asphaltene increases; hence, the amount of oil resistance factor increases. It can be concluded that permeability reduction increases as the value of α increases. It should be mentioned

that asphaltene deposition is a surface deposition phenomenon. Therefore, surface deposition is a predominant mechanism of physical deposition.

3.4 Effect of entrainment rate coefficient

Deposit re-entrainment and surface deposition proceed against each other. So, in most situations one of these two mechanisms is dominant, and the other one might be ignored. The results show that

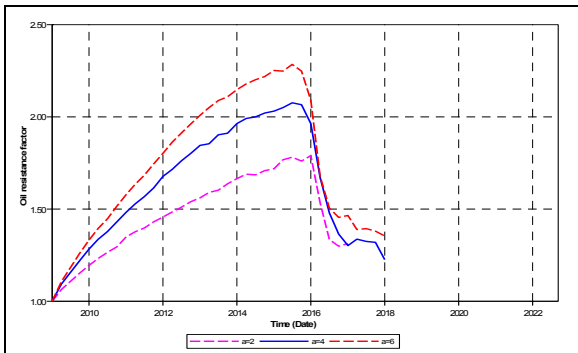


Figure 10. Effect of α on oil resistance factor.

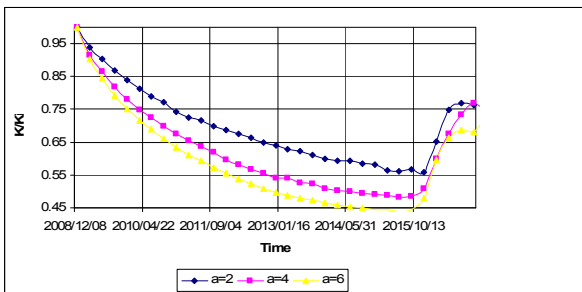


Figure 11. Effect of α on permeability reduction.

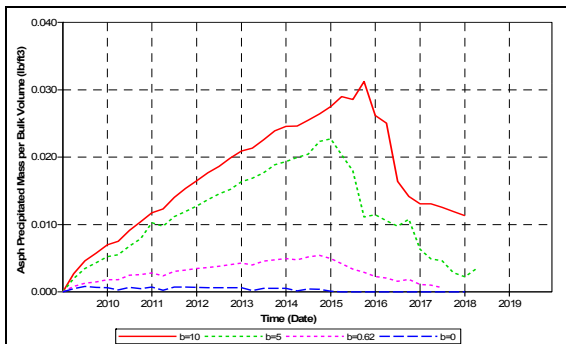


Figure 12. Effect of β on asphaltene precipitation.

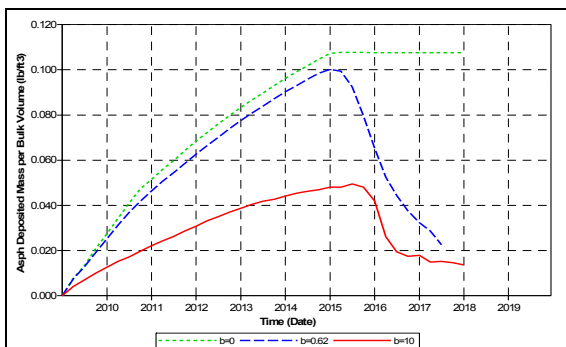


Figure 13. Effect of β on asphaltene deposition.

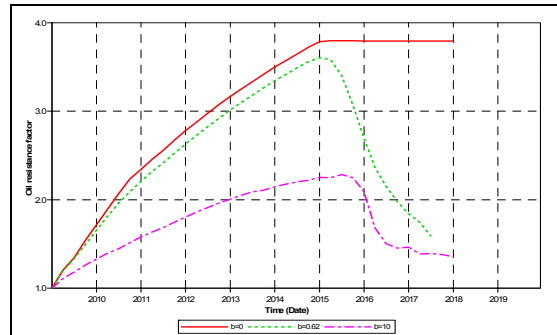


Figure 14. Effect of β on oil resistance factor.

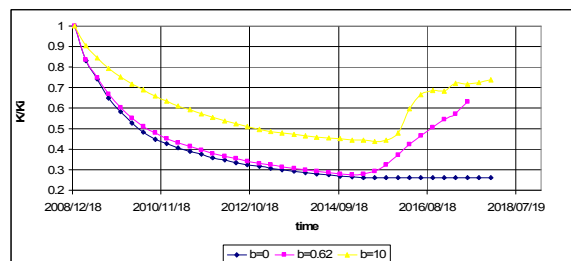


Figure 15. Effect of β on permeability reduction.

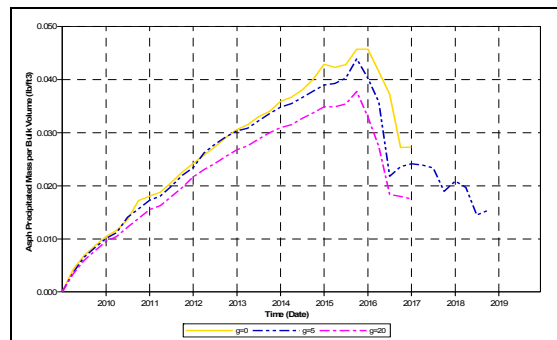


Figure 16. Effect of γ on asphaltene precipitation.

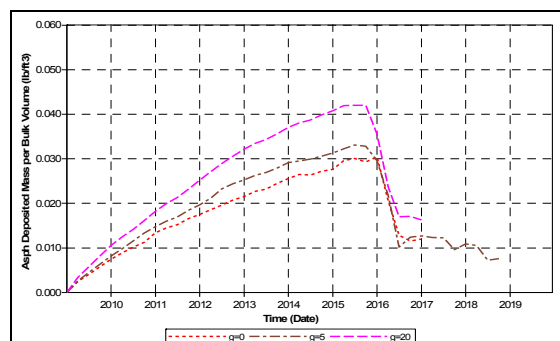


Figure 17. Effect of γ on asphaltene deposition.

Table 6. Cumulative asphaltene precipitation.

| Rate (bbl/day) | Cumulative asphaltene precipitation |
|----------------|-------------------------------------|
| 500 | 0.82 |
| 1000 | 0.73 |
| 1700 | 0.65 |
| 2000 | 0.62 |
| 5000 | 0.34 |

enhanced re-entrainment deposition allows flocculated asphaltene to change into precipitated asphaltene, or be dispersed into the oil phase (Figure 12). Figure 13 shows that the deposition of flocculated solid particles decreases with increasing β . Also, as a result of decreasing deposited asphaltene, the oil resistance factor decreases (Figure 14). In Figure 15, it can be seen that the permeability reduction decreases with increasing β .

3.5 Effect of pore throat plugging

The effects of pore throat plugging coefficient on asphaltene precipitation, deposition, oil resistance factor and permeability reduction are

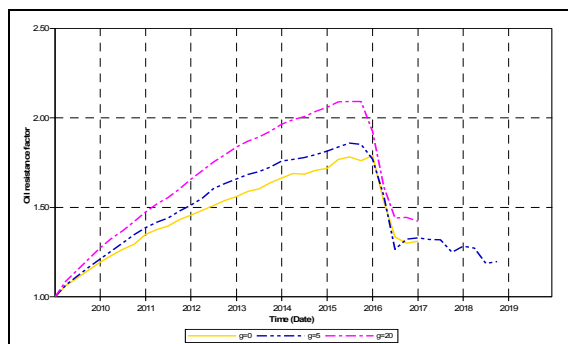


Figure 18. Effect of γ on oil resistance factor.

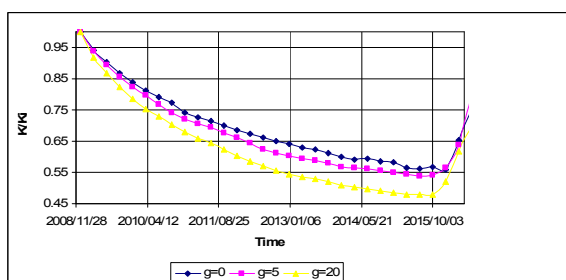


Figure 19. Effect of γ on permeability reduction.

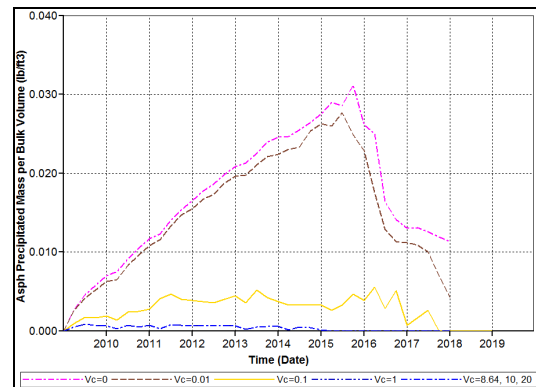


Figure 20. Effect of v_c on asphaltene precipitation.

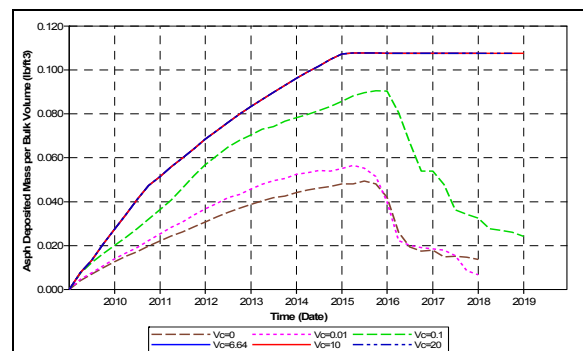


Figure 21. Effect of v_c on asphaltene deposition.

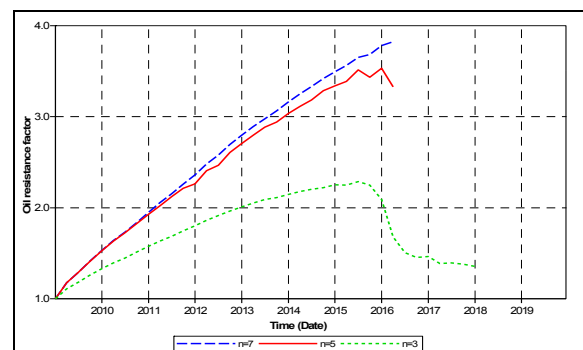


Figure 22. Effect of n exponent on oil resistance factor.

shown in Figures 16 through 19. The results show that when γ increases precipitated asphaltene decreases, whilst the deposition of flocculated solid particles at the pore throat increases and the oil resistance factor increases. These results can be explained in terms of filtration of the solid phase at the pore throat. Due to this mechanism, partial or total pore plugging is expected.

3.6 Effect of critical velocity

When v_c increases, precipitated asphaltene is decreased and deposited asphaltene increases (Figures 20 and 21). Asphaltene deposition

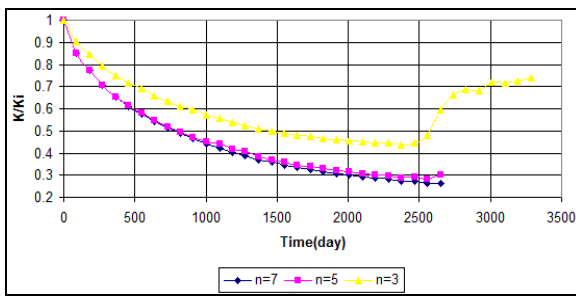


Figure 23. Effect of n exponent on permeability reduction.

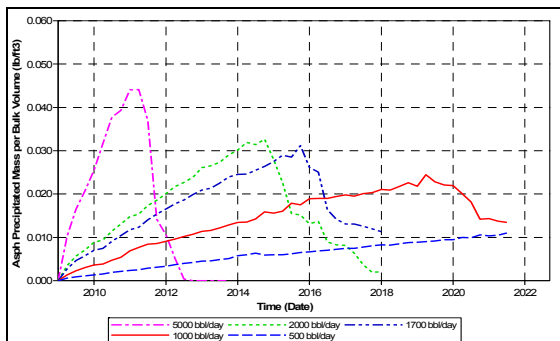


Figure 24. Effect of oil rate on asphaltene precipitation.



Figure 25. Effect of oil rate on cumulative asphaltene precipitation.

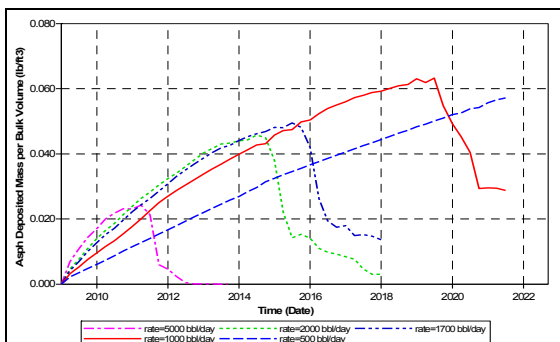


Figure 26. Effect of oil rate on asphaltene deposition.

continues when the interstitial velocity is less than v_c . At v_c , the entrainment mechanism is dominant, so the deposited asphaltene decreases.

3.7 Effect of oil resistance factor exponent

Civan et al. (1992) suggested the following empirical equation to express the reduction permeability:

$$Rf = \frac{k_i}{k} = \left(\frac{\phi_i}{\phi}\right)^n \quad (1)$$

Values of the exponent (n) range from 3 to 7 (Reis and Acock, 1994). Wang and Civan (2001) have reported an n value equal to 3. This value was used in all runs in this work. Figure 22 shows that the oil resistance factor increases when the oil resistance factor exponent increases; consequently, permeability reduction can also be expected (Figure 23).

3.8 Oil production rate

Asphaltene precipitation and deposition are rate-dependent mechanisms. Figure 24 shows that the increase on the rate of oil production results in early formation and higher maximum amount of

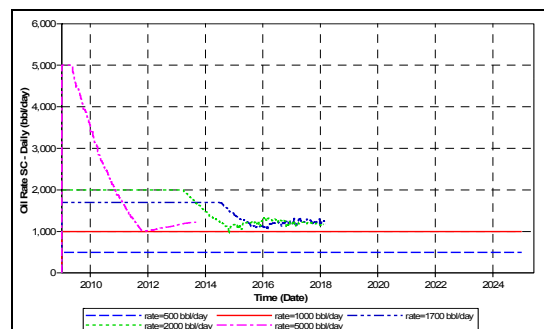


Figure 27. Variation of oil production at different oil rate versus time.

asphaltene precipitation. In addition, cumulative asphaltene precipitation decreases with increasing oil production rate (Figure 25). The amount of cumulative asphaltene precipitation for each oil production rate is given in Table 6.

Asphaltene deposition is highly sensitive to flow rate, hence any change in the flow rate affects the asphaltene deposition. By increasing oil production rate, lower levels of asphaltene deposition are observed (Figure 26). As a result, optimization of oil production rate can reduce asphaltene deposition.

Figure 27 shows that production rates up to 1000 bbl/day from any well will be uniform and steady through the history of production. However,

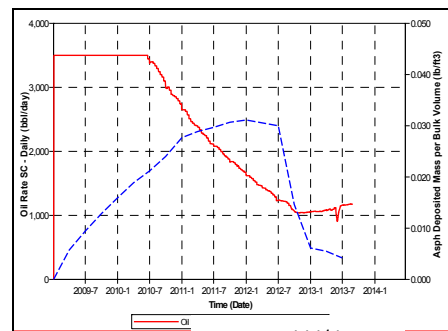
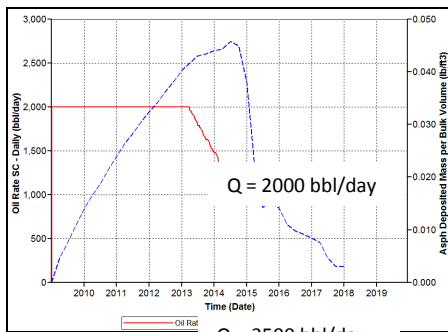
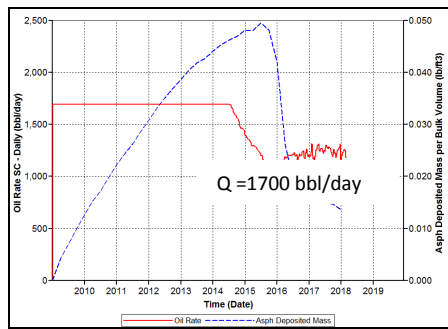


Figure 28. Effect of oil production rate on the extent of asphaltene deposition.

at higher rates (e.g. 2000 bbl/day), production declines during a short period of time down to 1000 bbl/day. The effect of oil production rate on asphaltene deposition is shown in Figure 28. As can be seen, at higher rates the deposition is reduced and occurs at the early stages of production.

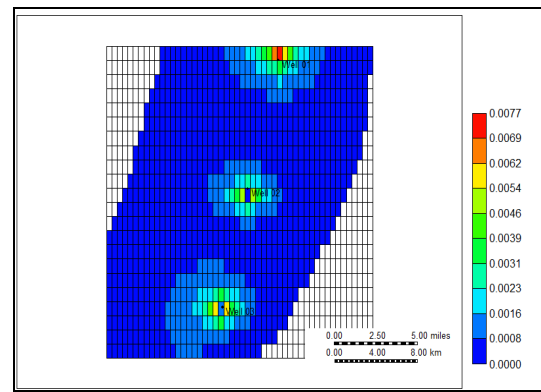


Figure 29. Zone of maximum probability of asphaltene precipitation.

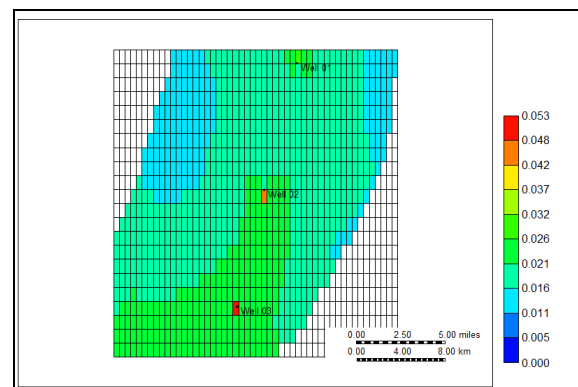


Figure 30. Zone of maximum probability of asphaltene deposition.

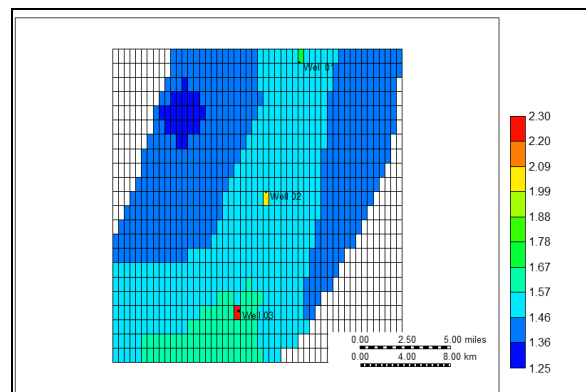


Figure 31. Zone of maximum probability of asphaltene oil resistance factor

3.9 Zone of maximum probability

Figures 29 through 31 illustrate the zone of maximum probability of asphaltene precipitation, deposition and oil resistance factor due to pressure depletion respectively. The observation shows that maximum amounts of asphaltene precipitation, deposition and oil resistance factor occur around the wells.

4. CONCLUSIONS

Based on the results of this work, the following conclusions are listed:

1. Maximum amounts of precipitation and deposition occur around the wellbore.
2. Maximum amount of precipitation was obtained at saturation pressure.
3. Observations showed that asphaltene precipitation/deposition is a rate-dependent mechanism. Increasing the oil production rate resulted in earlier, lower appearance of asphaltene deposition. Therefore optimization of oil production rate can reduce asphaltene deposition.
4. By increasing the surface deposition rate coefficient (α), asphaltene precipitation decreases. On the other hand, asphaltene deposition increases as α increases.
5. When the pore throat plugging rate coefficient increases, precipitated asphaltene decreases, whilst the deposition of flocculated solid particles at the pore throat increases; hence oil resistance factor increases.
6. This study has illustrated that controlling production rate is an important strategy in delaying asphaltene production in reservoirs where asphaltene problems are observed.

NOMENCLATURE

asph. = asphaltene (in Figures)
 GOR = Gas/oil ratio (SCF/STB)
 k_{12} = Conversion rate of precipitation to flocculation particles (1/day)
 k_{21} = Conversion rate of flocculation particles back to precipitation (1/day)
 k_i = Initial permeability (mD)
 k = Instantaneous permeability (mD)
 n = Exponent for calculation of permeability reduction due to solid deposition (dimensionless)
 P = Reservoir pressure (psia)
 P_b = Bubble-point pressure (psia)
 R_f = Oil resistance factor (dimensionless)
 T = Reservoir temperature ($^{\circ}$ F)
 v_c = Critical interstitial velocity (m/day, ft/day)
 α = Surface deposition rate constant (1/day)
 β = Entrainment rate constant (1/m, 1/ft)
 γ = Instantaneous pore throat plugging deposition rate constant (1/m, 1/ft)

δ = Snowball effect deposition constant (dimensionless)

ϕ_i = Initial porosity (dimensionless)

ϕ = Instantaneous porosity (dimensionless)

SI Conversion factors

1 D = 10^{-12} m²

1 ft = 0.3048 m

1 psia = 6.894757×10^3 Pa

1 STB = 0.1590168 m³

$^{\circ}$ F = 1.8 ($^{\circ}$ C) + 32

5. REFERENCES

Burce, F.K.; Nghiem, L.X. Modeling Asphaltene Precipitation and Deposition in a Compositional Reservoir Simulator, SPE 89437. In: SPE/DOE Fourteenth Symposium on Improved Oil Recovery, 2004, Tulsa, Oklahoma, U.S.A.

Civan, F. Evaluation and Comparison of the Formation Damage Models, SPE 23787. In: International Symposium on Formation Damage Control, 1992, Lafayette, Louisiana, U.S.A.

Garrouch, Ali A.; Feras, A. R. Predicting Asphaltene Deposition and Assessing Formation Damage, SPE 82258. In: SPE European Formation Damage Conference, 2003, Hague, Netherlands.

Hemanta, K.S. Can We Ignore Asphaltene in a gas injection Project for Light-oils? , SPE 84877. In: SPE International Improved Oil Recovery Conference, 2003, Asia Pacific, Kuala Lumpur.

Hirschberg, A.; DeJong, L.N.J.; Schipper, B.A.; Meijer, J.G. Influence of Temperature and Pressure on Asphaltene Flocculation. **Soc. Petrol. Eng.**, Vol.24, p.283-293, 1984.

Kharrat R., **Experimental and Modeling of Asphaltene Deposition for Iranian reservoirs, PEDC**, 2009.

Leontaritis, K.J.; Amaefule, J.O.; Charles, R.E. A Systematic Approach for the Prevention and Treatment of Formation Damage Caused by Asphaltene Deposition, SPE 23810. **SPE journal**, p.157-164, 1994.

Moghadasi J.; Kalantari-Dahaghi, A.M.; Gholami, V.; Abdi, R. Formation Damage Due to Asphaltene Precipitation Resulting From CO₂ Gas Injection in Iranian Carbonate Reservoirs, SPE 99631. In: SPE Europec/EAGE Annual Conference and Exhibition, 2006, Vienna, Austria.

Nghiem, L.X.; Dennis, A. Modeling Asphaltene Precipitation during Primary Depletion, SPE 36106. In: IV Latin American/Caribbean Pet. Eng. Conference, 23-26 April, 1996, Trinidad and Tobago.

Nghiem, L.X.; Kohse, B.F.; Farouq Ali, S.M.; Doan, Q. Asphaltene Precipitation: Phase Behavior Modeling and Compositional Simulation, SPE 59432. In: SPE Asia Pacific Conference on Integrated Modeling for Asset Management, 2000, Yokohama, Japan.

Reis J.C.; Acock A.M. Permeability Reduction Models for the Precipitation of Inorganic Solids in Berea Sandstone, In Situ (1994) 18, No. 3, 347-368.

Saad, F.A.; Fahed, A.; Al-Shammari, A.D. A Simplified Method to Predict Asphaltene Deposition in Oilwell Tubings: Field Case, SPE 84609. In: SPE Annual Technical Conference & Exhibition, Denver, 2003, Colorado, U.S.A.

Wang, Sh.; Civan, F. Productivity Decline of Vertical and Horizontal Wells by Asphaltene Deposition in Petroleum Reservoirs, SPE 64991. **International Symposium on Oilfield Chemistry**. Houston, Texas, 2001.